IEEE Access
Multidisciplinary | Rapid Review | Open Access Journal

Received 21 March 2024, accepted 1 April 2024, date of publication 5 April 2024, date of current version 12 April 2024.

Digital Object Identifier 10.1109/ACCESS.2024.3385495

RESEARCH ARTICLE

Denoising Method of Vibration Signal for CNC Machine Tool Multi-Component Feed System Based on Joint Analysis Method

JING TIAN[1], ENYU SHI[1], CHENGZHI FANG[1], YUSHEN CHEN[2], XIAOLIANG LIN[1], XIAOLEI DENG[1], XINHUA YAO[3,4], AND HONGYAO SHEN[3,4]

[1]Key Laboratory of Air-Driven Equipment Technology of Zhejiang Province, Quzhou University, Quzhou 324000, China
[2]College of Mechanical Engineering, Zhejiang University of Technology, Hangzhou 310032, China
[3]Key Laboratory of 3D Printing Process and Equipment of Zhejiang Province, School of Mechanical Engineering, Zhejiang University, Hangzhou 310027, China
[4]State Key Laboratory of Fluid Power and Mechatronic Systems, School of Mechanical Engineering, Zhejiang University, Hangzhou 310027, China

Corresponding authors: Xiaoliang Lin (lxl@qzc.edu.cn) and Xiaolei Deng (dxl@zju.edu.cn)

This work was supported in part by the National Natural Science Foundation of China under Grant 52175472 and Grant 62302263; in part by Zhejiang Provincial Natural Science Foundation of China under Grant LD24E050011, Grant LGG22E050031, and Grant ZCLTGS24E0601; in part by the Natural Science Foundation of Zhejiang Province for Distinguished Young Scholars under Grant LR22E050002; in part by the Science and Technology Plan Project of Quzhou under Grant 2021F010, Grant 2022K90, and Grant 2021K41; and in part by the National College Students' Innovation and Entrepreneurship Training Program of China under Grant 202311488011.

ABSTRACT The feed system is an important part of CNC machine tools, and its condition monitoring is mostly based on vibration signals measured by sensors. To remove the noise mixed in the signal, a joint denoising method based on variational mode decomposition (VMD), simple correlation analysis (SCA) and translation invariant wavelet (TIW) denoising is proposed in this paper. Firstly, the VMD parameters are adjusted adaptively by the Aquila Optimizer (AO) to meet the demand of signal decomposition from different components of feed system. Then, the intrinsic mode functions (IMFs) obtained after VMD processing are reconstructed based on correlation analysis to eliminate irrelevant information. Finally, the reconstructed signal is denoised by translation invariant wavelet to obtain the denoised signal. The feasibility and universality of the joint analysis method are verified by the denoising test of simulation signals and measured signals from a certain machine feed system. The results show that the joint analysis method has better denoising effect than some general denoising method, and it can satisfy the denoising requirement when processing signals from different components. Besides, the proposed method has the ability of adaptive denoising. Compared with other optimization algorithms, AO algorithm has better optimization accuracy and efficiency, which can provide good support for the universality of the joint analysis denoising method.

INDEX TERMS Aquila optimizer, machine tool, multi-component feed system, signal denoising, variational mode decomposition.

I. INTRODUCTION

A. RESEARCH BACKGROUND

The growth of the manufacturing sector has led to the popularization of precision CNC machine tools because to their fast processing rates, safety and dependability, high precision, and great efficiency. The feed system of precision CNC machine tools is composed of many complex components, which plays the role of precisely controlling the position of the tool and the workpiece [1]. Its positioning speed and accuracy determine the efficiency and quality of product manufacturing [2]. However, the state change of the feed system will affect the operation reliability of the whole machine. At present, the condition monitoring of machine tool feed system is mostly based on various sensors [3], [4], [5]. Among them, vibration signal analysis is one of the most common

The associate editor coordinating the review of this manuscript and approving it for publication was Diego Oliva.

ways to predict the development trend of machine tool state and judge the abnormal state of machine tool. However, when collecting machine tool vibration information, it is inevitable to mix various noises, such as human noise, environmental noise or noise generated by the sensor itself. It will cause the effective information contained in the original signal to be covered up, which is not conducive to further analysis [6]. Research indicates that denoising of collected vibration signals can enhance the accuracy of lifetime prediction [7] and fault diagnosis [8] of numerically controlled machine tools. For instance, Qian et al. [9] introduced a new domain generalization transfer method - the Relation Transfer Domain Generalization Network (RTDGN) - and applied it to fault diagnosis under varying noise levels. The results demonstrate that this algorithm significantly improves the accuracy of bearing fault diagnosis.

At present, the research of signal denoising algorithm has been relatively mature. Vibration signals collected from machine tool feed system are usually nonlinear and non-stationary [10], [11]. Fourier transform [12], as a denoising method based on linear systems, is generally not appropriate to process this kind of signals. Wavelet transform is frequently employed in the field of vibration signal denoising because of its nonlinear, locality and good time-frequency domain analysis characteristics. For example, Su et al. [13] denoised the vibration time domain signal of rotating machinery based on wavelet transform, effectively improving the fault identification ability.

As a time-frequency domain processing method [14], the most significant feature of empirical mode decomposition (EMD) is the proposal of the intrinsic mode function (IMF). The concept of IMF overcomes the problem that the wavelet basis function is not self-adaptive. However, its development and application are hindered by the serious problems of mode aliasing, end effect and so on. In 2009, Wu and Huang [15] proposed a signal analysis method based on improved EMD, namely ensemble empirical mode decomposition (EEMD). The method utilizes the EMD filter bank behavior and the statistical property of the uniform distribution of white noise spectrum to effectively suppress the mode aliasing caused by intermittent high-frequency components. Torres et al. [16] proposed the complete EEMD with adaptive noise (CEEMDAN). Because CEEMDAN can effectively solve the problem of white noise transmission from high frequency to low frequency, it is also widely used in signal denoising [17].

Compared with EMD and the improved EMD, variational mode decomposition (VMD) is an adaptive and completely non-recursive signal processing algorithm [18]. VMD has a complete mathematical model, and the IMF of the signal is obtained by solving the variational problem. Its decomposition quality is determined by the number of modes m and penalty coefficient μ. In order to optimize these two variables. Wang et al. [19] proposed the power information-guided variational modal decomposition (PIVMD). This method uses the envelope autoregressive (AR) power spectrum of the original vibration signal to derive the VMD parameters, so as to effectively extract the modal components of rolling bearing fault information. Li et al [20] proposed a fault information-guided VMD (FIVMD) method to extract the weak bearing repetitive transient. Intelligent optimization algorithm has been widely applied in the construction of optimal VMD model [21], [22]. Li et al. [23] used genetic algorithm (GA) to optimize variational mode decomposition (VMD) parameters and used it to extract fault feature information. Li et al. [24] imported snake optimization (SO) [25] into VMD for the first time, and proved that the proposed method has good performance in denoising ship radiated noise (SN).

Although the above denoising methods have achieved good results in some cases, there are still some problems: 1) The research of most denoising algorithms is limited to a single component, and the interaction between multiple components is not fully considered. Therefore, the denoising of multi-component vibration signal has certain research significance. 2) In a low SNR environment, the classical VMD, EMD and EMD improved algorithms are difficult to separate the noise components. Therefore, this paper considers using TIW to re-reduce the reconstructed signal, and removes the noise as much as possible on the basis of retaining the signal characteristics. Based on the above analysis, this paper constructs a new joint analysis denoising method AO-VMD-SCA-TIW.

B. RESEARCH CONTENTS

The proposed joint analysis denoising method consists of VMD, SCA and TIW. Among them, the important parameters m and μ of VMD are optimized by Aquila Optimizer (AO). This optimization algorithm takes m and μ as the basic attributes of population individuals, and the minimum envelope entropy of IMFs is used as the fitness function of the algorithm. Parameters with the best fitness were substituted into VMD to process the original signal, and the resulting IMFs were classified by correlation analysis. After the effective IMFs are selected for signal reconstruction, the reconstructed signal will be subsequently processed using TIW to obtain the denoised signal. In this paper, simulation signals and vibration signals of different components of the machine tool feed system were employed to test the proposed joint denoising method, so as to verify the effective and universality of the method.

The main novelties and contributions are summarized as follows: (1) The proposed algorithm not only has good de-noising effect on simulation signal and multi-component vibration signal of feed system, but also has certain universality. (2) Compared with EEMD and CEEMDAN, AO-VMD has better anti-mode aliasing ability by selecting the optimal the number of modes. In addition, due to the good mathematical properties of VMD, the impact features of the original signal can be better retained. (3) As a new meta-heuristic

algorithm, Aquila optimizer (AO) can provide more appropriate penalty coefficient μ and the number of modes m for VMD with high efficiency and accuracy.

The remaining chapters are arranged as follows: The second section, " fundamental theory of denoising", focuses on the VMD and TIW. In addition, AO is introduced to establish the optimal VMD model (AO-VMD). In the third section, "Joint denoising Algorithm", presents the fusion algorithm and provides an overview of the noise reduction process. In the fourth part, the harmonic signals containing impact and Gaussian white noise were constructed, and five different denoising algorithms are used to denoise respectively, to verify the effectiveness and advantages of the proposed method. In the fifth section, the application of the joint denoising method in the vibration signal of the machine tool multi-component feed system is introduced and verifies it has certain universality. The last section summarizes the whole paper and gives the conclusion.

II. FUNDAMENTAL THEORY OF DENOISING

A. VMD

VMD obtains the IMFs of each signal by solving variational optimization problems in the frequency domain. Different from the concept of IMF proposed by Huang et al in literature [14], VMD redefines the intrinsic mode functions of wireline broadband with more stringent constraints. The main steps are as follows: [26]

The mathematical expression of the m-th IMF component is as follow:

$$u_m(t) = \mathrm{A}_m(t)\cos(\Phi_m(t)) \tag{1}$$

where, $\Phi_m(t)$ is the signal's instantaneous phase and $\mathrm{A}_m(t)$ is the envelope amplitude spectrum of signal $u_m(t)$.

Next, the constrained variational model is constructed. Firstly, the analytic signal $u(t)$ is obtained by Hilbert transformation of $u_m(t)$. The exponential harmonic signal $e^{j\phi_m(t)}$ is added to each IMF to adjust the center frequency of the analytic signal. Each IMF is then translated into the base band. Finally, the bandwidth is estimated by analyzing the Gaussian smoothness of the signal. The following constrained variational problem can be obtained:

$$\begin{cases} \min\limits_{\{u_m\},\{\omega_m\}} \{\sum\limits_m ||\partial_t[(\mathrm{d}(t)+\dfrac{j}{\pi t})^* u_m]\, e^{-j\omega_m t}||_2^2\} \\ st.\ \sum\limits_m u_m(t) = f \end{cases} \tag{2}$$

where, IMFs and the corresponding center frequencies are denoted by $\{u_m\}$ and $\{\omega_m\}$ respectively. The derivative with respect to time is denoted by $\mathrm{d}(t)$, and the Dirichlet function is denoted by ∂_t.

To solve this constraint problem, the constraint optimization problem can be equivalently transformed into an unconstrained optimization problem using the augmented Lagrangian function, and then solved by alternating direction method of multipliers (ADMM). Alternately update u_m^{n+1}, ω_m^{n+1} and λ^{n+1} to search the best solution to the problem mentioned above [27].

The penalty factor μ and the total number of modes m will affect the quality of VMD decomposition. The Aquila optimizer will be used in this paper to determine the two parameter values.

B. AO-VMD

The Ao is a novel intelligent optimization algorithm inspired by the hunting process of the Aquila in North America. Its has strong solving ability, fast convergence speed and strong stability. In this paper, the AO can be employed to determine the parameter values of VMD adaptively to achieve the best decomposition effect in different conditions. The process of the algorithm is as follows: [28]

Step1: Population initialization

The AO is a swarm based intelligent algorithm, so the first step is to build a matrix $\boldsymbol{W}$ to randomly initialize the population position:

$$\begin{aligned} \boldsymbol{W}_{ij} &= rand \times (\boldsymbol{VB}_j - \boldsymbol{MB}_j) + \boldsymbol{MB}_j, \\ & i = 1, 2, \ldots, N_j = 1, 2, \ldots, Dim \end{aligned} \tag{3}$$

where, N represents the population size and Dim represents the dimension of the search space.

Step2: The global optimal solution is obtained via four population behaviors

(1) Expand the search: The Aquila flock will soar upward to expand the search area, which can be summarized as follows:

$$\boldsymbol{W_1}(t+1) = \boldsymbol{W}_{\mathrm{best}}(t) \times (1-\frac{t}{T}) + (\boldsymbol{W}_{\mathrm{M}}(t) - \boldsymbol{W}_{\mathrm{best}}(t) \times rand)$$

$$\boldsymbol{W}_{\mathrm{M}}(t) = \frac{1}{N}\sum_{i=1}^{N} \boldsymbol{W}_i(t), \quad \forall j = 1, 2, \ldots Dim \tag{4}$$

where, $\boldsymbol{W}(t)$ and $\boldsymbol{W}(t+1)$ represent the individual positions in the t and t+1 iterations respectively; $\boldsymbol{W}_{\mathrm{best}}(t)$ and $\boldsymbol{W}_{\mathrm{M}}(t)$ represent the optimal individual position and the average position of the population when the algorithm is iterated to t times, respectively. T represents the total number of iterations.

(2) Narrow the scope: When Aquila birds spot prey, they will circle above the target. This process that can be expressed as:

$$\boldsymbol{W}_2(t+1) = \boldsymbol{W}_{\mathrm{best}}(t) \times \mathrm{Levy}(D) + \boldsymbol{W}_R(t) + (y-x) \times rand \tag{5}$$

where, $\boldsymbol{W}_R(t)$ represent a random solution of N loaded values after a contraction exploration iteration, and $Levy(D)$ is Lévy flight distribution (LFD), and x and y represent the shape of the flight.

$$\begin{cases} \mathrm{Levy}(D) = s \times \dfrac{\mu \times \sigma}{|\nu|^{\frac{1}{\beta}}} \\ \sigma = (\dfrac{G(1+\beta) \times \sin\frac{\pi\beta}{2}}{G(\frac{1+\beta}{2}) \times \beta \times 2^{\frac{\beta-1}{2}}}) \end{cases} \tag{6}$$

where, μ and v are random numbers taken from [0, 1]; G(x) is the gamma function, and $\beta = 1.5$.

(3) Extend development: When the Aquila birds are ready to land and attack, the vertical descent approach will be taken to initial attack. The position function is updated as follows:

$$\boldsymbol{W}_3(t+1) = (\boldsymbol{W}_{\text{best}}(t) - \boldsymbol{W}_{\text{M}}(t) \times \alpha) - rand + ((\boldsymbol{VB} - \boldsymbol{MB}) \times rand + \boldsymbol{MB}) \times \delta \quad (7)$$

where, α and δ are the adjustment parameters selected from 0 to 1.

(4) Shrink development: Aquila birds attack the prey with a certain randomness, and the behavior of walking and grabbing prey can be expressed as follows:

$$\boldsymbol{W}_4(t+1) = \text{QE}(t) \times \boldsymbol{W}_{best}(t) - (H_1 \times \boldsymbol{W}(t) \times rand) - H_2 \times \text{Levy}(D) + rand \times H_1 \quad (8)$$

where, QE(t) represents the quality function used to balance the search strategy. H_1 represents the random movements of the Aquila birds in the process of tracking prey. H_2 represents the linearly decreasing flight slope value, the range is [0, 2]. The QE(t), H_1 and H_2 can be calculated as follows:

$$\begin{aligned} \text{QE}(t) &= t^{\frac{2\times rand-1}{(1-T)^2}} \\ H_1 &= 2 \times rand - 1 \\ H_2 &= 2 \times (1 - \frac{t}{T}) \end{aligned} \quad (9)$$

In this paper, μ and m are optimized by the AO, and the minimum envelope entropy of the IMF is selected as its fitness function. It's calculated by the following formula:

$$\begin{cases} E_r = -\sum_{k=1}^{N} r_k \lg r_k \\ r_k = f(r) / \sum_{k=1}^{N} f(r) \end{cases} \quad (10)$$

where, E_r is the envelope entropy which is the normalized form of $f(r)$, and $f(r)$ is the envelope signal obtained by Hilbert demodulation of the IMF component.

The sparse feature of the original signal can be represented by the envelope entropy. The envelope entropy is greater when there is more noise and less feature information in the IMF. Therefore, the AO can adaptively adjust the result of variational mode decomposition by calculating the envelope entropy of the IMF. The optimal parameter combination is the one that produces the most characteristic information while producing the least noise.

C. TIW

In wavelet denoising methods, the threshold method is widely used and can achieve good denoising effect. The threshold denoising method broadly used in engineering is realized by setting the threshold v. Its mathematical expression is as follows:

$$\bar{c} = \begin{cases} sign(c \times \left[\left|c^2\right| - v^2\right]^{\frac{1}{2}}), & |c| \geq v \\ 0, & |c| \leq v \end{cases} \quad (11)$$

where, c is the wavelet coefficient and $\bar{c}$ is the wavelet coefficient after quantization. $sign()$ is a symbolic function. v is the threshold, and $v = \sqrt{2 \lg L}$,where L represents the signal length.

However, when the matching degree between the signal features and the features of the wavelet base elements is too low, pseudo-Dibbs will be generated by using the threshold method. The translation invariant wavelet denoising can effectively suppress this phenomenon. In this method, n times of cyclic translation is adopted, and the signal after each translation is denoised by threshold method. Then the result after denoising is averaged. It is the basic idea of the translation invariant wavelet denoising method of ''translation - denoising - average'' [29]. The idea can be expressed as:

$$\overline{\text{T}}(x_t, (\text{S}_h)_{h\in H_n}) = \text{AVE}_{h\in H_n} \frac{1}{\text{S}_h}(\text{T}(\text{S}_h(x_t))) \quad (12)$$

where, x_t represents a signal. S_h represents a time-domain translation of the signal x_t by h units. h is a positive integer whose value range is $H_n = \{h : 0 \leq h < n\}$. T represents that the threshold method is used for signal denoising, and AVE means ''average''.

III. JOINT ANALYSIS DENOISING METHOD

Based on the above basic theory, a joint denoising method named AO-VMD-SCA-TIW is proposed. The process of AO-VMD-SCA-TIW is as follows:

Step1: The VMD parameters are optimized with the Aquila optimizer (AO-VMD):

(1) Set basic parameters of AO: population size =10, iteration number =10, search space of m is [2, 10], and the search space of μ is [50,2000].

(2) Initialize the population position $\boldsymbol{W}$, and the algorithm starts looping at $t = 1$.

(3) Calculate the average population location, and the position $\boldsymbol{W}_1$(t+1), $\boldsymbol{W}_2$(t+1), $\boldsymbol{W}_3$(t+1), $\boldsymbol{W}_4$(t+1) were updated successively according to the each phase.

(4) Calculate the respective fitness according to the updated position of the Aquila birds, so as to find the optimal fitness value and the position of the corresponding individual.

(5) The fitness value of the current optimal individual is compared with that of the optimal individual obtained in the t generation, and the position of the better individual is retained.

(6) Determine whether the termination conditions are met. If not, repeat steps (4)-(6). If yes, jump out of the loop and get the best decomposition parameter [m, μ].

Step2: The VMD algorithm based on the optimal parameters can process the noisy signal and obtain m IMF components. The simple correlation analysis technique is used to provide theoretical basis for signal reconstruction. The correlation between each IMF and the original signal can be analyzed to judge whether it can be discarded as irrelevant information. The better the correlation between the two variables, the closer the absolute value of the correlation

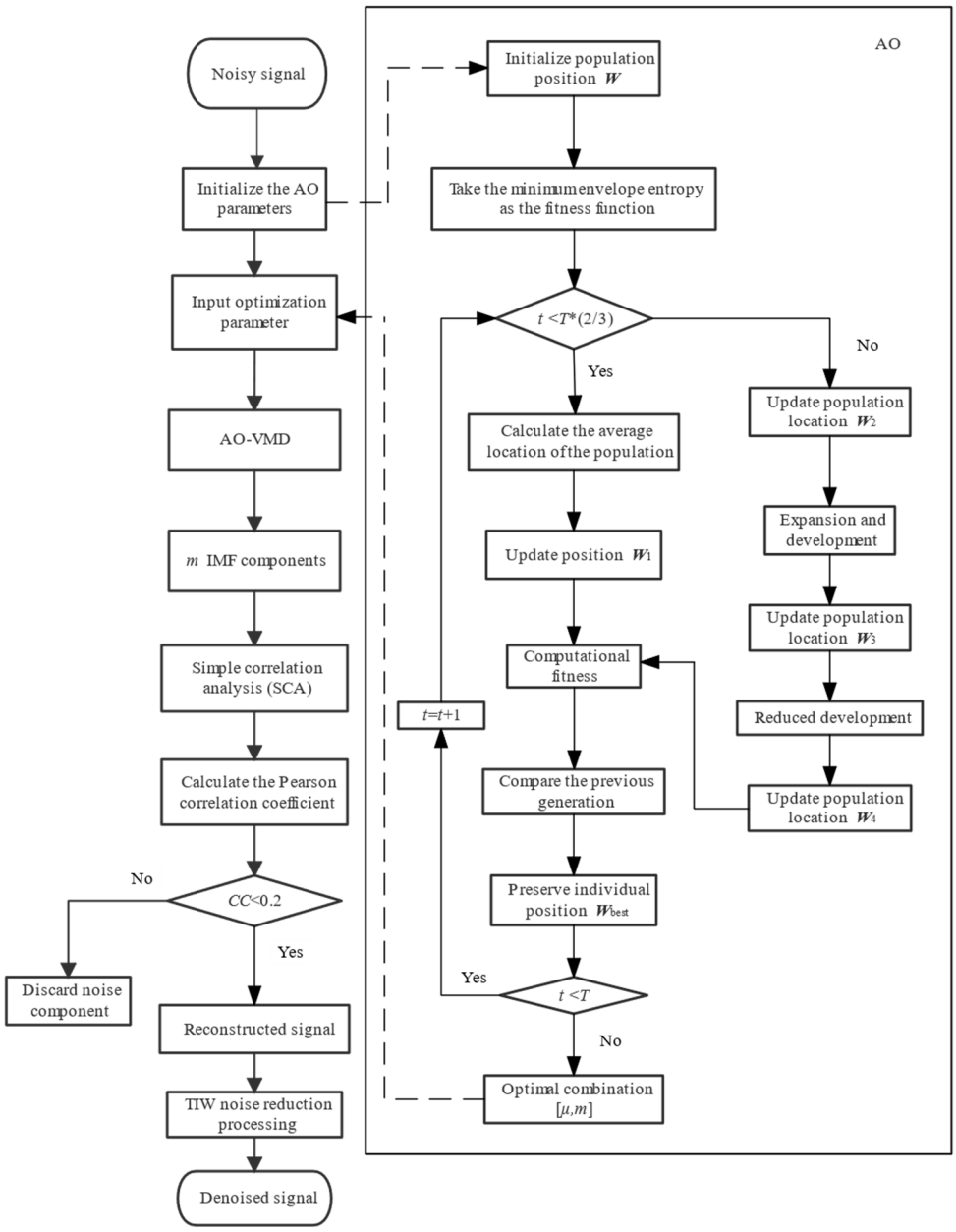

FIGURE 1. The flow chart of the joint denoising method AO-VMD-SCA-TIW.

coefficient is to 1. Its mathematical expression is as follows:

$$CC_{xy} = \frac{\sum_{m=1}^{n}(X_m - \overline{X})(Y_m - \overline{Y})}{\sqrt{\sum_{m=1}^{n}(X_m - \overline{X})^2}\sqrt{\sum_{m=1}^{n}(Y_m - \overline{Y})^2}} \tag{13}$$

where, X represents the original signal and Y_m represents the m-th IMF component obtained via VMD. CC_{xy} represents the Pearson correlation coefficient between the original signal and IMF.

Step 3: According to [30], the threshold of Pearson correlation coefficient CC_{xy} was set as 0.2. The IMF will be regarded as noise component if its correlation coefficient is below the threshold. The reconstructed signal can be obtained by combining the remaining components after eliminating these noise components.

Step 4: The reconstructed signal is further denoised by TIW to obtain the final denoised signal. The flow chart of the joint analysis denoising method AO-VMD-SCA-TIW is shown in Fig. 1.

IV. SIMULATION SIGNAL TEST

A. SIMULATION SIGNAL CONSTRUCTION

In order to verify the availability of AO-VMD-SCA-TIW, the denoising experiment of the simulated signal was carried out

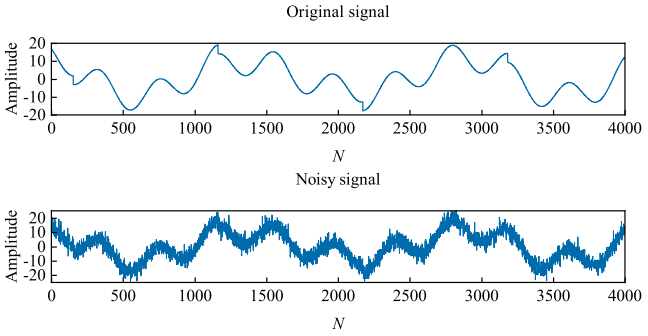

FIGURE 2. Diagram of simulation signal generation.

first. The components in the machine tool feed system are usually affected by a variety of environmental factors and will be affected by irregular shocks, so the intensity and frequency of the noise source will constantly change. In this section, considering the actual working conditions, a pulse signal and Gaussian white noise were added to a stationary signal. The definition of simulation signal X is as follows:

$$\begin{aligned} X_1 &= \mathrm{A}_1 \sin(2\pi f_1 t + \cos(2\pi f_2 t)) + \mathrm{A}_2(\mathrm{e}^{\mathrm{i}\omega t} + \mathrm{e}^{-\mathrm{i}\omega t}) \\ X_2 &= \mathrm{pulstran}(T, D, \text{'tripuls'}, 5, 1) \\ X &= \mathrm{awgn}(X_1 + X_2, n_i, 'measured') \end{aligned} \tag{14}$$

where, $A_1 = 8$ and $A_2 = 10$ represent the amplitude of the signal; $f_1 = 0.25$ and $f_2 = 0.005$ represent the frequency of the signal; X_2 is a pulse signal; T represents the sampling time and D represents the sampling interval; X represents the simulation signal after adding Gaussian white noise with specified signal-to-noise ratio (SNR); n_i represents Gaussian white noise of different intensity. In this paper, Gaussian white noise with SNR of -9dB, -5dB, 5dB and 9dB was added to the original signal respectively for simulation.

According to equation (14), X is the signal containing noise, and X_1+X_2 is the original signal. Taking the simulation signal containing 9db Gaussian white noise as an example, both the original signal and noisy signal are displayed in Fig.2.

B. SIMULATION SIGNAL DENOISING

In this paper, root mean square error (RMSE) and SNR were employed to evaluate the denoising effect of AO-VMD-SCA-TIW. The mathematical expression is as follows:

$$\begin{aligned} RMSE &= \sqrt{\frac{1}{n}\sum_{i=1}^{n}(\mathrm{f}(l) - \mathrm{s}(l))^2} \\ SNR &= 10\log\left(\frac{\sum_{i=1}^{N}\mathrm{S}^2(l)}{\sum_{i=1}^{N}[\mathrm{f}(l) - \mathrm{s}(l)]^2}\right) \end{aligned} \tag{15}$$

where, l is the length of the signal; $\mathrm{f}(l)$ is the signal after AO-VMD-SCA-TIW denoising, and $\mathrm{s}(l)$ is the original signal. The smaller the RMSE value and the larger the SNR value, the better the denoising effect.

TABLE 1. Initial parameters of optimization algorithm.

Parameter	Value or region
Number m of IMFs	$m \in [2,10], m \in Z$
Penalty factor μ	$\mu \in [1000,5000], m \in Z$
The maximum iteration numbe T	10
The size of population	10

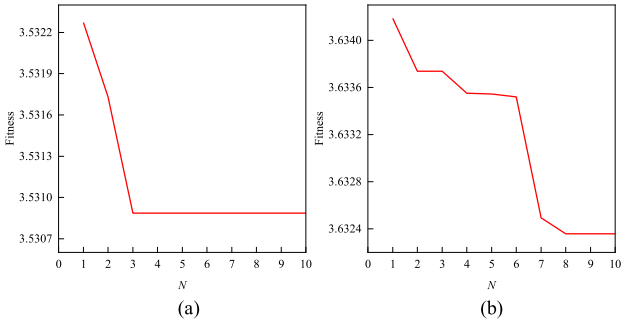

FIGURE 3. Iterative process of the two algorithms. (a) AO-VMD-SCA-TIW. (b) GA-VMD-SCA-TIW.

To verify the superiority of AO-VMD-SCA-TIW, this paper compared it with GA-VMD-SCA-TIW, VMD-SCA-TIW, CEEMDAN-SCA-TIW, and EEMD-SCA-TIW. Among them, the former uses the genetic algorithm (GA) proposed by Holland to replace the Aquila optimizer to achieve the purpose of parameter optimization. VMD-SCA-TIW employs VMD to replace the optimized VMD. After several simulations, the number of modes m = 5 and penalty coefficient $\mu = 4000$ were artificially selected. The latter two use EEMD and CEEMDAN to replace VMD.

Four groups of simulation signals were obtained by adding four kinds of white Gaussian noise and pulse signals with different intensities to the original signal. AO-VMD-SCA-TIW, GA-VMD-SCA-TIW, VMD-SCA-TIW, CEEMDAN-SCA-TIW, EEMD-SCA-TIW were used to denoise the noisy signal respectively. Table 1 shows the initialization parameters of the fusion optimization algorithm. Fig. 3 shows the different iterative processes based on AO-VMD-SCA-TIW and GA-VMD-SCA-TIW methods for signals with SNR of 9dB.

As can be seen from the above figure, both algorithms completed convergence within ten iterations. The minimum fitness of GA was 3.6323 and the minimum fitness of AO was 3.5308. The smaller the envelope entropy, the less noise contained in the IMF component, so it can be drawn that AO had a better optimization effect. Furthermore, as seen in Fig.5, the convergence speed of AO was faster: its convergence was completed at the third iteration, while GA was completed at the eighth iteration. In terms of computational efficiency, the running time of AO was 106.89 seconds, while the running time of GA was 1403.028 seconds, which shows that AO has better efficiency.

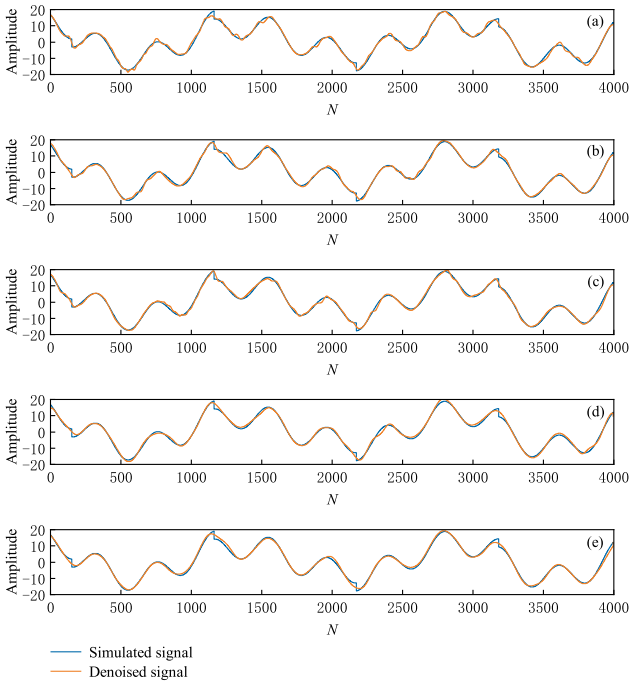

FIGURE 4. Comparison of denoising effect of five algorithms with a SNR of 5dB. (a) AO-VMD-SCA-TIW. (b) GA-VMD-SCA-TIW. (c)VMD-SCA-TIW. (d) CEEMDAN-SCA-TIW. (d)EEMD -SCA-TIW.

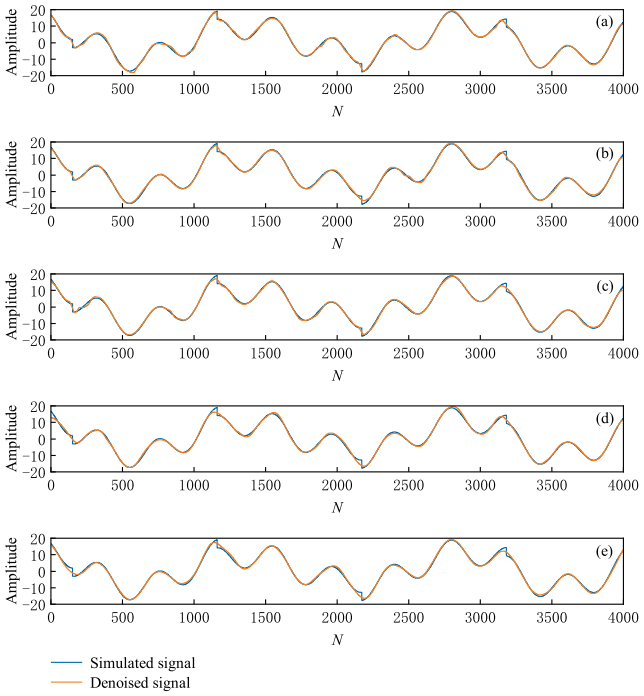

FIGURE 5. Comparison of denoising effect of five algorithms with a SNR of 9dB. (a) AO-VMD-SCA-TIW. (b) GA-VMD-SCA-TIW. (c)VMD-SCA-TIW. (d) CEEMDAN-SCA-TIW. (d)EEMD -SCA-TIW.

In order to verify the advantages of VMD in this algorithm, this paper compared VMD with EEMD and CEEMDAN. Taking the simulation signals with a SNR of 5db and 9db as an example, the processes AO-VMD-SCA-TIW, GA-VMD-SCA-TIW, VMD-SCA-TIW, EEMD-SCA-TIW and CEEMDAN-SCA-TIW were used for denoising, respectively. Fig. 4 and 5 show the actual denoising results under different methods.

The above figures clearly shows that the denoised signal following AO-VMD-SCA-TIW processing has the best matching performance with the original signal. According to the denoising results, the reconstructed signal after variational mode decomposition can retain the pulse signal in the original signal. The fundamental reason is that they have different definitions of IMF. IMF in EMD needs to meet two conditions: First, within the entire data segment, the number of extreme points and the number of zero crossing points must be equal or no more than one difference. Second, at any time, the average value of the upper envelope formed by the local maximum point and the lower envelope formed by the local minimum point are zero. These will result in the shock signal being separated as a factor affecting the mean envelope. The IMF of VMD is defined as formula (1), which has a perfect mathematical model and will not be affected by shock features.

Table 2 details the processing effects of the five denoising methods discussed above on the four sets of simulation signals. Furthermore, the effects of combined denoising with TIW and denoising with simply signal reconstruction are compared, where '-' indicates that the signal is reconstructed based only on simple correlation analysis.

Through vertical analysis of the table, it can be found that with the increase of SNR, the denoising effects of various methods are all improving. This shows that similar joint analysis denoising methods are easier to deal with signals with less noise. The horizontal analysis of the data in the table shows that AO-VMD-SCA-TIW has the highest SNR value and the lowest RMSE value under the same SNR, indicating that it has the best denoising effect.

In the process of denoising, the optimization algorithm will find the optimal VMD parameters to reduce the mutual interference between different mode functions as much as possible. When AO-VMD-SCA-TIW and GA-VMD-SCA-TIW are compared under different situations, the denoising effect of AO-VMD-SCA-TIW is superior to that of GA-VMD-SCA-TIW. This is because under the same premise of using VMD for signal decomposition, the AO can get more appropriate decomposition parameters, so as to further improve the anti-mode aliasing ability. Comparing the noise reduction effect of AO-VMD-SCA-TIW and VMD-SCA-TIW under different conditions, the noise reduction effect of AO-VMD-SCA-TIW is better than that of VMD-SCA-TIW. Because EEMD adds Gaussian white noise during signal decomposition, even if it cancels the extra white noise after ensemble averaging, residual Gaussian white noise in the reconstructed signal is unavoidable, resulting in mode aliasing. In summary, the AO-VMD-SCA-TIW method proposed in this paper has advantages in processing simulated signals.

TABLE 2. Denoising effect of five methods on noisy signals.

Groups	Index		AO-VMD-SCA	GA-VMD-SCA	VMD-SCA	CEEMDAN-SCA	EEMD-SCA
-9dB	SNR	+TIW	**9.4423**	7.8543	5.3011	5.2151	5.1401
	RMSE		**3.0541**	3.7004	4.6459	4.9195	5.0665
	SNR	-	**9.2234**	7.6531	5.2957	5.1931	5.0997
	RMSE		**3.1242**	3.8034	4.9014	5.0231	5.1657
-5dB	SNR	+TIW	**13.1632**	12.4814	10.5750	11.8583	7.7966
	RMSE		**1.9884**	2.1507	2.6786	2.3107	3.6883
	SNR	-	**13.1399**	12.2712	9.6188	11.8260	7.7056
	RMSE		**1.9937**	2.2024	2.9903	2.3193	3.7271
5dB	SNR	+TIW	**26.5595**	21.2533	21.0037	23.2428	22.8288
	RMSE		**0.7949**	0.7834	0.8063	0.6230	0.6535
	SNR	-	**19.3840**	21.0503	18.4723	18.8663	14.1226
	RMSE		**0.9715**	0.8019	1.0790	1.0312	1.7804
9dB	SNR	+TIW	**24.7975**	24.2779	24.5489	25.5301	25.0631
	RMSE		**0.5209**	0.5530	0.5361	0.4233	0.4402
	SNR	-	**24.0832**	23.4480	23.7217	22.7390	22.5956
	RMSE		**0.5656**	0.6085	0.5896	0.6602	0.6712

(a)

(b)

FIGURE 6. Feed system signal acquisition experiment.

V. APPLICATION OF MULTI-COMPONENT EXPERIMENTAL DATA IN FEED SYSTEM

In this section, the AO-VMD-SCA-TIW method was applied to the actual working conditions. To test the universality of the proposed method for vibration signals denoising, vibration signals were collected from different components in the feed system. The experimental site is a machining shop, where the personnel turnover rate is high and multiple machine tools are running at the same time. There were a lot of noise sources in the experimental environment, which affected the accurate acquisition of vibration signals.

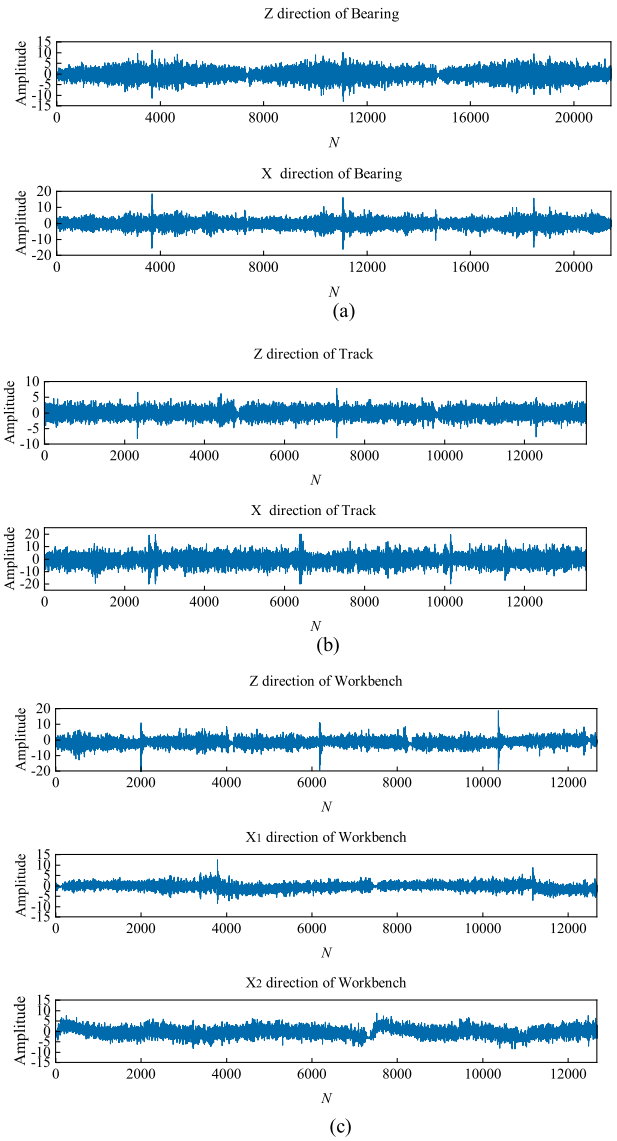

FIGURE 7. Selected experimental data.

The experimental equipment was composed of IEPE piezoelectric sensors, a data acquisition device and a computer. The acquisition device is shown in Fig. 6(a), and the distribution points of the vibration signal acquisition experiment for the multi-component feed system are shown in Fig. 6(b). 8 measuring points were arranged on the workbench, 4 measuring points were arranged on the bearing seat, and 7 measuring points were arranged on the guide rail to collect the signals in all directions of different components as far as possible.

There were two working conditions were designed: the motor speed of 4000 rpm and 5000 rpm, respectively. The sampling frequency of the signal acquisition equipment was all maintained at 1kHz and the machine table maintained round-trip movement. Before the test starts, the collected vibration signal was screened, that is, the signal with obvious signal characteristics and clear waveform was retained, and the similar signal removed. The vibration signal acquisition

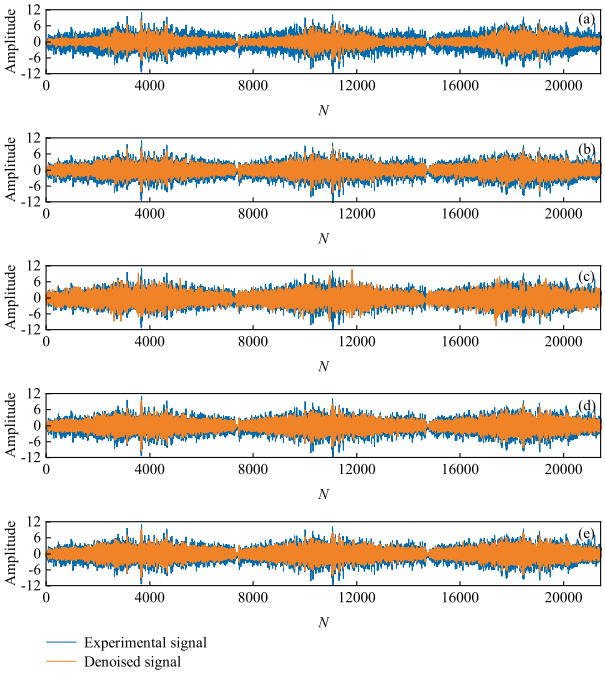

FIGURE 8. Denoising effect on the vibration signals of bearing seat in the X direction. (a)AO-VMD-SCA-TIW (b)GA-VMD-SCA-TIW. (c)VMD-SCA-TIW. (c) CEEMDAN -SCA-TIW. (d)EEMD-SCA-TIW.

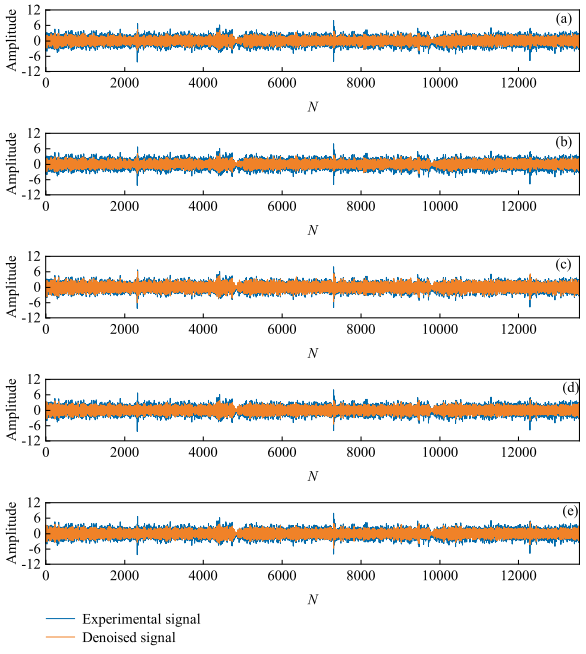

FIGURE 9. Denoising effect on the vibration signals of track seat in the X direction: (a) AO-VMD-SCA-TIW. (b) GA-VMD-SCA-TIW. (c)VMD-SCA-TIW. (d) EEMD-SCA-TIW. (e) CEEMDAN-SCA-TIW.

results of the selected components are shown in Fig. 7. (T1 and T7 measuring points on the track, B2 and B4 measuring points on the bearing seat, and W2, W5 and W7 measuring points on the workbench).

In this paper, in order to preserve the complete characteristics of signals, the length of the signal interception is different

TABLE 3. NRR values corresponding to the five methods.

Working condition	Measuring point	AO-VMD-SCA-TIW	GA-VMD-SCA-TIW	VMD-SCA-TIW	CEEMDAN-SCA-TIW	EEMD-SCA-TIW
4000r/min	Track X	6.6128	6.1133	4.3512	3.3215	1.0291
	Track Z	5.6355	5.4310	3.2477	1.1804	0.3219
	Bearing block X	7.7003	5.1655	3.3512	2.2834	2.0326
	Bearing block Z	5.3342	4.9112	2.5361	1.6630	0.8356
	Workbench X1	6.6124	6.0812	4.5123	2.5416	1.0411
	Workbench X2	6.3120	6.1204	4.3513	2.2512	1.1221
	Workbench Z	5.6891	5.6702	4.1453	1.4561	0.9411
5000r/min	Track X	5.0315	4.9952	2.9932	2.1503	1.0035
	Track Z	5.0012	4.8531	3.0643	0.8231	0.8342
	Bearing block X	5.3013	5.1655	3.6612	2.2834	2.0326
	Bearing block Z	5.0121	4.1102	2.0163	1.0044	0.8156
	Workbench X1	5.6533	5.3412	3.5631	1.1884	0.2219
	Workbench X2	5.4501	5.2042	3.2215	1.5304	0.3208
	Workbench Z	4.5911	4.4202	2.5361	1.1641	0.3401

for different components. As shown in Fig.7, the vibration signal of each component has a certain regularity, which is because the machine maintained a round-trip movement. The signals of different components have significant differences in amplitude and baseline offset. Therefore, it is of great significance to denoise the vibration signal of the machine tool feed system with multiple components.

The evaluation criteria such as SNR and RMSE mentioned in the previous section are only applicable when the pure signal is known. However, the real pure signal cannot be obtained in the process of collecting vibration signal in real environment. As a result, the noise rejection ratio (NRR) was employed as the criterion for evaluating the denoising effect of experimental signals [31]. The greater the NRR value, the more effective the denoising performance. Its mathematical expression is as follows:

$$\mathrm{NRR} = 10\left(\lg\sigma_1^2 - \lg\sigma_2^2\right) \tag{16}$$

where, σ_1 and σ_2 are the variance of the original experimental signal and the signal after denoising, respectively.

Fig. 8 and Fig. 9 shows the denoising effect of five different denoising algorithms on the vibration signals of two components in the X direction. Table 3 shows the comparison of denoising effect of five denoising methods on different experimental signals under different working conditions.

From the Fig.8 and the Fig.9, it can be found that the five methods have reduced the burr in the experimental signal to some level, and the signal features are well retained. Concurrently, the experimental signal's baseline drift is simultaneously adjusted to a lower level.

The vertical comparison of the data in the Table 3 reveals that the denoising effect of the same method on multiple groups of signals will change due to different components and working conditions. Through horizontal analysis, it can be concluded that AO-VMD-SCA-TIW has the best denoising effect for the same group of signals. It is indicated that AO-VMD-SCA-TIW has good performance in denoising vibration signals of each component of the machine tool feed system, which verifies the universality of the method.

VI. CONCLUSION

For the complex multi-component feed systems in the machine tool, this paper proposes a joint analysis method AO-VMD-SCA-TIW to decrease the noise mixed in the vibration signal. The simulation results demonstrate that the proposed AO-VMD-SCA-TIW method achieves the minimum RMSE value and the highest SNR value. Based on the feed system's multi-component experimental results, it is obvious that AO-VMD-SCA-TIW produces higher NRR values when denoising vibration signals generated by different components.

In conclusion, the joint denoising algorithm can effectively eliminate the noise in the signal collected by the sensor, and has wide applicability in the denoising of vibration signals from multi-component feed system. This technology is expected to be applied to the fault diagnosis and life prediction of the feed system of CNC machine tools and can lay a foundation for the subsequent information fusion.

CONFLICTS OF INTEREST

The authors have no conflicts of interest to declare that are relevant to the content of this article.

AUTHOR CONTRIBUTIONS

All authors reviewed the manuscript. Jing Tian: writing-reviewing and editing; Enyu Shi: validation, writing-original draft; Xiaolei Deng, Yushen Chen, Chengzhi Fang: conceptualization; Xiaoliang Lin, Xinhua Yao, Hongyao Shen: resources.

ACKNOWLEDGMENT

(Jing Tian and Enyu Shi are co-first authors.)

REFERENCES

[1] H. Yang, Z. Wang, T. Zhang, and F. Du, "A review on vibration analysis and control of machine tool feed drive systems," *Int. J. Adv. Manuf. Technol.*, vol. 107, nos. 1–2, pp. 503–525, Feb. 2020.

[2] H. Zhang, J. Zhang, H. Liu, T. Liang, and W. Zhao, "Dynamic modeling and analysis of the high-speed ball screw feed system," *Proc. Inst. Mech. Eng., B, J. Eng. Manuf.*, vol. 229, no. 5, pp. 870–877, Jun. 2014.

[3] Y. Zhou and W. Xue, "A multisensor fusion method for tool condition monitoring in milling," *Sensors*, vol. 18, no. 11, p. 3866, Nov. 2018.
[4] X. Li, P. K. Venuvinod, and M. K. Chen, "Feed cutting force estimation from the current measurement with hybrid learning," *Int. J. Adv. Manuf. Technol.*, vol. 16, no. 12, pp. 859–862, Oct. 2000.
[5] S. Abdi, E. Abdi, H. Toshani, and R. McMahon, "Vibration analysis of brushless doubly fed machines in the presence of rotor eccentricity," *IEEE Trans. Energy Convers.*, vol. 35, no. 3, pp. 1372–1380, Sep. 2020.
[6] C. Fang, Y. Chen, X. Deng, X. Lin, Y. Han, and J. Zheng, "Denoising method of machine tool vibration signal based on variational mode decomposition and whale-tabu optimization algorithm," *Sci. Rep.*, vol. 13, no. 1, p. 1505, Jan. 2023.
[7] L. Wan, K. Chen, Y. Li, Y. Wu, Z. Wang, and C. Li, "A novel remaining useful life prediction method based on CEEMDAN-IFTC-PSR and ensemble CNN/BiLSTM model for cutting tool," *IEEE Access*, vol. 10, pp. 2182–2195, 2022.
[8] H. Hang, W. Xue, J. Yao, and Y. Wang, "Fault diagnosis of NC machine tool feed system based on graph theory diagnosis method and wavelet packet transform," *J. Vib. Shock*, vol. 41, no. 15, pp. 130–137, 2022.
[9] Q. Qian, J. Zhou, and Y. Qin, "Relationship transfer domain generalization network for rotating machinery fault diagnosis under different working conditions," *IEEE Trans. Ind. Informat.*, vol. 19, no. 9, pp. 9898–9908, Sep. 2023.
[10] H. Liu and M. Han, "A fault diagnosis method based on local mean decomposition and multi-scale entropy for roller bearings," *Mechanism Mach. Theory*, vol. 75, pp. 67–78, May 2014.
[11] M. R. A. A. Abad, A. Moosavian, and M. Khazaee, "Wavelet transform and least square support vector machine for mechanical fault detection of an alternator using vibration signal," *J. Low Freq. Noise, Vib. Act. Control*, vol. 35, no. 1, pp. 52–63, Mar. 2016.
[12] H.-C. Lin and Y.-C. Ye, "Reviews of bearing vibration measurement using fast Fourier transform and enhanced fast Fourier transform algorithms," *Adv. Mech. Eng.*, vol. 11, no. 1, Jan. 2019, Art. no. 168781401881675.
[13] N. Su, X. Li, and Q. Zhang, "Fault diagnosis of rotating machinery based on wavelet domain denoising and metric distance," *IEEE Access*, vol. 7, pp. 73262–73270, 2019.
[14] N. E. Huang, Z. Shen, S. R. Long, M. C. Wu, H. H. Shih, Q. Zheng, N.-C. Yen, C. C. Tung, and H. H. Liu, "The empirical mode decomposition and the Hilbert spectrum for nonlinear and non-stationary time series analysis," *Proc. Roy. Soc. London. Ser. A, Math., Phys. Eng. Sci.*, vol. 454, no. 1971, pp. 903–995, Mar. 1998.
[15] Z. Wu and N. E. Huang, "Ensemble empirical mode decomposition: A noise-assisted data analysis method," *Adv. Adapt. Data Anal.*, vol. 1, no. 1, pp. 1–41, Jan. 2009.
[16] M. E. Torres, M. A. Colominas, G. Schlotthauer, and P. Flandrin, "A complete ensemble empirical mode decomposition with adaptive noise," in *Proc. IEEE Int. Conf. Acoust., Speech Signal Process. (ICASSP)*, Prague, Czech Republic, May 2011, pp. 4144–4147, doi: 10.1109/ICASSP.2011.5947265.
[17] L. Bai, Z. Han, Y. Li, and S. Ning, "A hybrid de-noising algorithm for the gear transmission system based on CEEMDAN-PE-TFPF," *Entropy*, vol. 20, no. 5, p. 361, May 2018.
[18] H. Hu, Y. Ao, H. Yan, Y. Bai, and N. Shi, "Signal denoising based on wavelet threshold denoising and optimized variational mode decomposition," *J. Sensors*, vol. 2021, pp. 1–23, Jul. 2021.
[19] X. Wang, J. Shi, and J. Zhang, "A power information guided-variational mode decomposition (PIVMD) and its application to fault diagnosis of rolling bearing," *Digit. Signal Process.*, vol. 132, Jan. 2023, Art. no. 103814.
[20] Q. Ni, J. C. Ji, K. Feng, and B. Halkon, "A fault information-guided variational mode decomposition (FIVMD) method for rolling element bearings diagnosis," *Mech. Syst. Signal Process.*, vol. 164, Feb. 2022, Art. no. 108216.
[21] Y. Li, B. Tang, X. Jiang, and Y. Yi, "Bearing fault feature extraction method based on GA-VMD and center frequency," *Math. Problems Eng.*, vol. 2022, pp. 1–19, Jan. 2022.
[22] J. Li, W. Luo, M. Bai, and M. Song, "Fault diagnosis of high-speed rolling bearing in the whole life cycle based on improved grey wolf optimizer-least squares support vector machines," *Digit. Signal Process.*, vol. 145, Feb. 2024, Art. no. 104345.
[23] J. Li, W. Chen, K. Han, and Q. Wang, "Fault diagnosis of rolling bearing based on GA-VMD and improved WOA-LSSVM," *IEEE Access*, vol. 8, pp. 166753–166767, 2020, doi: 10.1109/ACCESS.2020.3023306.
[24] Y. Li, B. Tang, S. Jiao, and Q. Su, "Snake optimization-based variable-step multiscale single threshold slope entropy for complexity analysis of signals," *IEEE Trans. Instrum. Meas.*, vol. 72, pp. 1–13, 2023, doi: 10.1109/TIM.2023.3317908.
[25] F. A. Hashim and A. G. Hussien, "Snake optimizer: A novel meta-heuristic optimization algorithm," *Knowl.-Based Syst.*, vol. 242, Apr. 2022, Art. no. 108320.
[26] K. Dragomiretskiy and D. Zosso, "Variational mode decomposition," *IEEE Trans. Signal Process.*, vol. 62, no. 3, pp. 531–544, Feb. 2014, doi: 10.1109/TSP.2013.2288675.
[27] C. Wang, H. Li, G. Huang, and J. Ou, "Early fault diagnosis for planetary gearbox based on adaptive parameter optimized VMD and singular kurtosis difference spectrum," *IEEE Access*, vol. 7, pp. 31501–31516, 2019, doi: 10.1109/ACCESS.2019.2903204.
[28] C. Liu and J. Zhen, "Diagonal loading beamforming based on Aquila optimizer," *IEEE Access*, vol. 11, pp. 69091–69100, 2023, doi: 10.1109/ACCESS.2023.3293403.
[29] J. Chen, Z. Li, J. Pan, G. Chen, Y. Zi, J. Yuan, B. Chen, and Z. He, "Wavelet transform based on inner product in fault diagnosis of rotating machinery: A review," *Mech. Syst. Signal Process.*, vols. 70–71, pp. 1–35, Mar. 2016.
[30] Y. Li, Y. Li, X. Chen, and J. Yu, "Research on ship-radiated noise denoising using secondary variational mode decomposition and correlation coefficient," *J. Vibroeng.*, vol. 19, no. 2, pp. 1185–1192, Mar. 2018.
[31] H. Shang, J. Yuan, Y. Wang, and S. Jin, "Application of wavelet footprints based on translation-invariant in of partial discharge signal detection," *Trans. China Electrotech*, vol. 28, no. 10, pp. 33–40, Oct. 2013.

JING TIAN received the M.S. degree from Zhejiang University of Technology, China, in 2008.

She is currently a Lecturer of mechanical engineering with Quzhou University. Her research interests include dynamic reliability testing and evaluation of intelligent equipment, condition monitoring, and fault diagnosis of key components of mechanical systems.

ENYU SHI was born in Zhejiang, China, in 2003. He is currently pursuing the bachelor's degree in mechanical engineering with Quzhou College, Quzhou University, with a focus on mechatronic engineering and automation.

His research interests include vibration and fault diagnosis.

CHENGZHI FANG was born in Zhejiang, China, in 2002. He is currently pursuing the bachelor's degree in intelligent manufacturing engineering with Quzhou College, Quzhou University.

He is good at thermal error modeling of key machine tool systems. He has good data analysis and the ability to build machine-learning models.

YUSHEN CHEN is currently pursuing the degree with Zhejiang University of Technology. His research interests include CNC equipment and automation technology.

XIAOLIANG LIN received the M.Sc. degree from Northeast Forestry University, China, in 2017.

He is currently an Experimentalist with Quzhou University. His main research interests include digital design and manufacturing technology of CNC equipment.

XIAOLEI DENG received the Ph.D. degree from Zhejiang University, China, in 2014.

He is currently a Professor with the College of Mechanical Engineering, Quzhou University. His main research interests include CNC equipment and automation technology, and digital design and manufacturing technology.

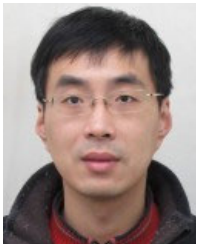

XINHUA YAO received the bachelor's and Ph.D. degrees in computer science and technology from Zhejiang University, in July 2001 and September 2006, respectively.

From October 2006 to November 2008, he was a Postdoctoral Researcher with the Postdoctoral Mobile Station of Mechanical Engineering, Zhejiang University. In December 2008, he was hired as a Lecturer and promoted to an Associate Professor, in December 2011. He is mainly engaged in intelligent manufacturing, industrial internet, composite additive manufacturing, and other fields of research, involving professional knowledge including computer and automation, control, and machinery.

HONGYAO SHEN received the bachelor's and Ph.D. degrees in mechanical manufacturing and automation from the Department of Mechanical Engineering, Zhejiang University, in 2005 and 2010, respectively.

He was a Postdoctoral Researcher with the Control Science and Engineering Postdoctoral Mobile Station, Zhejiang University, in 2010, and a Postdoctoral Researcher with the Manufacturing Automation Laboratory, The University of British Columbia, Canada, from 2011 to 2012. Since 2013, he has been teaching with the School of Mechanical Engineering, Zhejiang University, and promoted to a Professor, in 2021. His main research interests include high-performance numerical control machining and additive manufacturing technology. He has conducted special research on complex surface cutter path generation, multi-axis trajectory planning, online error compensation, metal additive manufacturing, green additive manufacturing, and additive and subtractive manufacturing.